Gyroid Structures and Morphological Control in Binary Blends of Polystyrene-*block*-polyisoprene Diblock Copolymers

Shinichi Sakurai,* Hiroshi Irie, Hideo Umeda, and Shunji Nomura

Department of Polymer Science and Engineering, Kyoto Institute of Technology, Sakyo-ku, Kyoto 606, Japan

Hee Hyun Lee and Jin Kon Kim

Department of Chemical Engineering and Polymer Research Institute, Pohang University of Science and Technology, Pohang, Kyungbuk 790-784, Korea

Received April 7, 1997; Revised Manuscript Received November 17, 1997

ABSTRACT: We report the morphology and phase behaviors of binary blends of polystyrene-*block*-polyisoprene (SI) copolymers, which were studied by a small-angle X-ray scattering (SAXS) technique. The neat SI copolymers employed in this study have almost the same molecular weights but different volume fractions of polystyrene block ($\phi_{PS} = 0.26$ and 0.65). Blends with various overall volume fractions of polystyrene block ($\bar{\phi}_{PS}$), ranging from 0.41 to 0.60, were prepared from these two SI copolymers. It was found that the morphology can be controlled by adjusting $\bar{\phi}_{PS}$. For the blends with $0.57 \leq \bar{\phi}_{PS} \leq 0.60$, the morphological transition from lamellae to gyroid phases was observed upon increasing the temperature. We present an experimentally determined phase diagram for the blend by plotting χZ vs $\bar{\phi}_{PS}$, where χ is the interaction parameter and Z is the reduced value of the total degree of polymerization of the block copolymer.

I. Introduction

Binary blends of diblock copolymers, $[(A-B)_\alpha + (A-B)_\beta]$, have been found to exhibit curious morphological behaviors which are not attained in neat block copolymers or in blends of a block copolymer and a homopolymer.[1−7] These characteristics of binary blends of diblock copolymers are ascribed to the situation that long and short polymer chains which are anchored to the interface are coexisting in the same microdomain space.[7] Many research groups have investigated the order−disorder transition,[8−10] morphology and phase behavior,[10−14] and morphological transition in binary blends of diblock copolymers.[15] Some groups have investigated the phase behavior of the binary blend of diblock copolymers where each constituent block copolymer has the same composition; namely, the volume fraction of block A in the block copolymer α is the same as that in the block copolymer β, but each copolymer has a different total molecular weight.[2,5] Others have highlighted effects of asymmetry in the composition of the constituent block copolymers, where the total molecular weight of the block copolymer α is almost the same as that of the block copolymer β.[4,7] An anomalous temperature behavior of the lamellar domain spacing, that is, the lamellar domain spacing *increases* with increasing temperature, was observed in the latter blend,[7] where the constituent components (polystyrene and polyisoprene) in each block copolymer exhibit an upper critical solution temperature (UCST) behavior.

The primary interest of a binary blend of block copolymers is to control the morphology by changing the overall composition of one block in the blend. This can be done simply by changing the added amount of each block copolymer. This method becomes a time-saving way to control the morphology as compared with others, for instance, the synthesis of a block copolymer with a targeted composition. One of the most important points in the preparation of the binary blend consisting of diblock copolymers is to prevent macroscopic phase separation. Very recently, one member of our group demonstrated that rapid solvent evaporation from the cast solution of the binary blend is an effective way to obtain the homogeneous microdomain structures.[7] As compared to a neat diblock copolymer, the binary blend of diblock copolymers exhibits some characteristic morphological behaviors; for instance, bicontinuous domains can be more easily formed in the blend than in a neat diblock copolymer. Figure 1 schematically shows two different morphologies found in the binary blend of the block copolymer α, $(A-B)_1$, and the block copolymer β, $(A-B)_2$. Here, block copolymers α and β are assumed to have complementary volume fractions of the block A, i.e., $f(\alpha) = 1 - f(\beta)$, and the volume fraction of the block copolymer α in the blend is slightly larger than 0.5. In this case, the overall composition of the block A in the blend, $\bar{\phi}_A$, is slightly smaller than 0.5. We assume that the lamellar and gyroid morphologies are thermodynamically ensured for this composition at lower and higher temperatures, respectively. As illustrated in Figure 1a, the A and B block chains are stretched out in the direction normal to the interface due to the strong segregation between A and B at a lower temperature. In this situation, the energetic contribution due to strong segregation overcomes the contribution of the conformational entropy. Hence, the lamellar structure is formed even when there is intradomain segregation of α blocks. When the temperature is raised, the contribution of the conformational entropy dominates due to a decrease of the segregation between A and B block chains. As a consequence, the cluster of α components forms a column of the A microdomain,

* To whom correspondence should be addressed. E-mail: shin@ipc.kit.ac.jp.

S0024-9297(97)00471-3 CCC: $15.00
Published on Web 01/07/1998

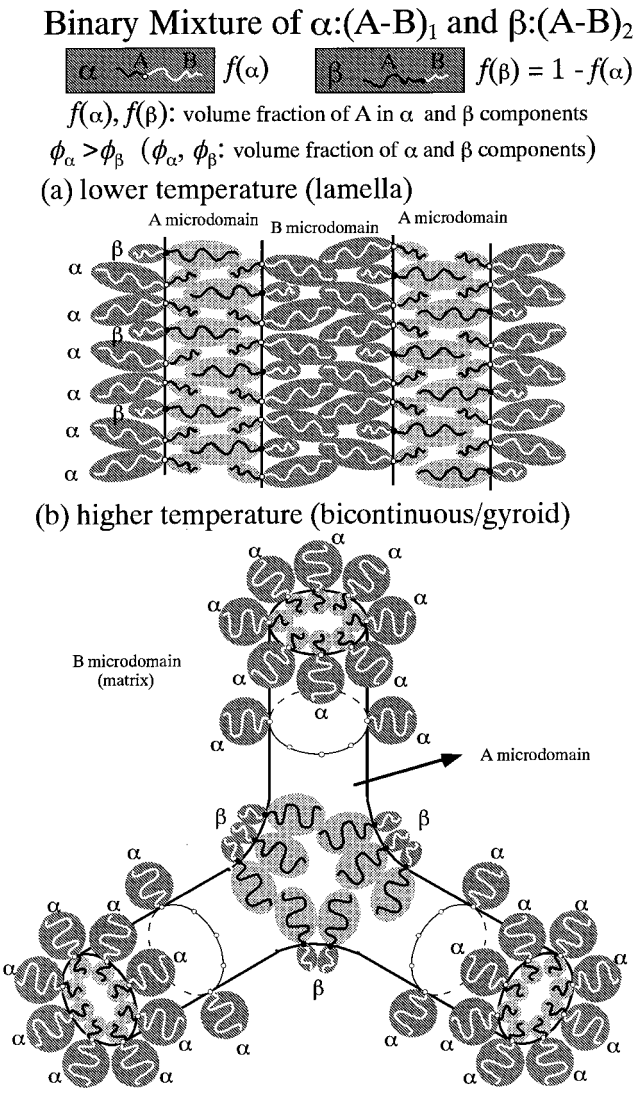

Figure 1. Schematic representation to demonstrate some characteristics of binary blends of diblock copolymers α, $(A-B)_1$, and β, $(A-B)_2$. Here, block copolymers α and β are assumed to have complementary volume fractions of the block A, i.e., $f(\alpha) = 1 - f(\beta)$, and the volume fraction of the block copolymer α in the blend is slightly larger than 0.5. In this case, the overall composition of the block A in the blend, $\overline{\phi_A}$, is slightly smaller than 0.5. These illustrations aim to explain that significant characteristics of the binary blends of diblock copolymers arise from the situation that long and short polymer chains which are anchored to the interface are coexisting in the same microdomain space. The intradomain segregation of the β blocks can reduce an energy barrier for the thermotropic transition from lamella in part a to bicontinuous domain (gyroid) in part b. It is assumed that the lamellar and gyroid morphologies are thermodynamically ensured for this composition at lower and higher temperatures, respectively.

and, in turn, further intradomain segregation takes place. The β components which are extracted from the $(\alpha + \beta)$ mixture due to the intradomain segregation participate in branching of the A microdomains. Thus, such a bicontinuous morphology as illustrated in Figure 1b is formed at a higher temperature. Note that the transition between Figure 1a and b is governed, in principle, by thermodynamics. However, the intradomain segregation of the β blocks can reduce an energy barrier for the transition. This is one of the interesting aspects of binary blends of diblock copolymers. The studies on morphological behaviors may reveal significant characteristics of the binary blends of diblock copolymers, arising from the situation that long and short polymer chains which are anchored to the interface are coexisting in the same microdomain space.

Table 1. Sample Characteristics

code name	ϕ_{PS}[a]	M_n[b] ($\times 10^3$)	M_w/M_n[c]	Z[d]	microstructure of PI[e] (mol %) cis-1,4	trans-1,4	3,4
SIZ-3	0.65	26.1	1.06	302	61	33	6
SIZ-4	0.26	24.5	1.05	302	73	20	7

[a] Volume fraction of polystyrene, analyzed by NMR. [b] Number-average molecular weight measured by membrane osmometry. [c] Heterogeneity index of molecular weight, measured by GPC. (M_w denotes the weight-average molecular weight.) [d] Reduced value of total degree of polymerization. [e] Analyzed by NMR.

Although theoretical predictions suggest the possibility that the morphological transition from one microdomain to the other is thermoreversible for a neat block copolymer with an appropriate f,[16,17] experimental confirmation for such a morphological transition is rather limited, except for special block copolymers.[15,18−26] Presumably, the occurrence of the morphological transformation sometimes needs to overcome an enormous energy barrier, even if it is thermodynamically favored. Careful studies are required to examine the thermoreversible morphological transition. As stated above, it is expected that the transition is more easily achieved in the binary blends of diblock copolymers than in the neat block copolymers. Very recently, we reported a thermally induced morphological transition from lamellar (L) and gyroid (G) phases, which was revealed with small-angle X-ray scattering (SAXS) and transmission electron microscopy (TEM).[15] The sample used was a binary blend of polystyrene-*block*-polyisoprene (SI) diblocks, with the overall polystyrene (PS) content (volume fraction of PS, $\overline{\phi_{PS}}$), being 0.58. The L and G phases were observed at lower and higher temperatures, respectively. Although the thermoreversibility of the transition was not confirmed, the stabilities of lamellar and of gyroid phases were confirmed at the lower and higher temperatures, respectively. The transition from G to L can be considered to be kinetically prohibited more than the transition from L to G in the binary blends of diblock copolymers.

In the present paper, a thermally induced morphological transition from L to G and further to a cylindrical morphology is reported for the binary blends with various values of $\overline{\phi_{PS}}$, ranging from 0.41 to 0.60. For the blend with $\overline{\phi_{PS}} = 0.60$, cylinder microdomains were observed when annealing was done at higher temperatures, while the G phase existed when annealing was done at slightly lower temperatures. We present an experimentally determined phase diagram for the blend in the plot of χZ vs $\overline{\phi_{PS}}$, where χ is the interaction parameter between styrene and isoprene segments, and Z is the reduced value of a total degree of polymerization of the block copolymer.

II. Experimental Section

The molecular characteristics of two neat SI copolymers, SIZ-3 and SIZ-4, employed in the blend are listed in Table 1. The two SI copolymers have similar total molecular weights in terms of Z but different volume fractions of PS block in the block copolymer, ϕ_{PS}. Z denotes the reduced value of the total degree of polymerization of the copolymer, where effects of differences in the segment sizes for PS and PI are corrected for. Z is defined as

$$Z = (v_{PS}N_{PS} + v_{PI}N_{PI})/v_0 \quad (1)$$

with $v_0 = (v_{PS}v_{PI})^{1/2}$. v_0, v_{PS}, and v_{PI} are molar volumes of the reference cell, PS, and PI segments, respectively. Note here that the values of v_K used were 107.2 and 81.9 cm^3/mol for PS and PI, respectively, which were evaluated from the values of mass density, 0.969 g/cm^3 for PS and 0.830 g/cm^3 for PI at 413 K.[27] N_K designates the degree of polymerization for K block (K = PS or PI). Samples were prepared as follows: after dissolving a predetermined amount of two neat block copolymers of SIZ-3 and SIZ-4 into toluene with a total polymer concentration of ca. 5 wt %, the solution was poured into a Petri dish, and the solvent was gradually evaporated. After complete removal of the solvent, the as-cast samples were further annealed at several temperatures for long times (at least 20 h) in a vacuum oven, followed by quenching into an ice/water mixture to freeze morphological structures with the assistance of vitrification of the PS block.

The SAXS measurements with synchrotron radiation were conducted at the BL-10C beam line of the Photon Factory (PF) in the Institute of High Energy Physics, Japan. The light source of this beam line is a bending magnet. The primary beam was monochromatized with a couple of Si(111) crystals at the wavelength of 0.1488 nm (the photon energy of X-rays is 8.33 keV), and then it was focused on a detector plane by a Pt-coated bent cylindrical mirror. A one-dimensional position-sensitive proportional counter (PSPC) was used to detect intensities and was set 1.9 m from the sample position (the direction of the 1d PSPC is vertical). Typical exposure time was chosen to be 5 min for our block copolymer samples of about 1 mm thickness. We subtracted the scattering intensity of an empty cell with two pieces of thin poly(ethylene terephthalate) films from that of samples by taking into account the transmittance of X-rays through the samples. The contribution of the thermal diffuse scattering (TDS) arising from the density fluctuations was further subtracted. Here, we approximated that the intensity at the high q region, where the scattering intensity is independent of q, is identical to the intensity level of TDS. q is the magnitude of the scattering vector, defined as

$$q = (4\pi/\lambda) \sin(\theta/2) \quad (2)$$

where λ and θ are the wavelength of the incident X-rays and the scattering angle, respectively. The obtained scattering intensities were not converted to absolute units. Some synchrotron SAXS measurements were conducted at the 3C2 beam line at the Pohang Light Source (PLS), Korea.[28] The primary beam was monochromatized with double Si(111) crystals at the wavelength of 0.1594 nm (the photon energy of X-ray is 7.76 keV), and then it was focused on a detector plane by a bent cylindrical mirror. A one-dimensional position-sensitive detector (diode-array PSD, Princeton Instruments Inc., Model ST-120) with each diode at a distance of 25 μm was used. All the SAXS measurements for annealed samples were done at room temperature.

III. Results and Discussion

Figure 2 shows the SAXS profiles (log $I(q)$ vs q) measured at room temperature for neat block copolymers of SIZ-3 annealed at 150 °C for 2 h and of SIZ-4 annealed at 110 °C for 26 h, where $I(q)$ denotes the scattering intensity. To avoid overlap, the intensity for SIZ-3 was shifted vertically by a factor of 3. It can be seen that (i) for neat SIZ-3, at least three peaks are observed, and the q values marked by arrows are assigned to $1:3^{1/2}:7^{1/2}$, which correspond to diffraction peaks of hexagonally packed cylinders ($[(h^2 + hk + k^2)^{1/2}]$,[29] and (ii) for neat SIZ-4, two higher-order peaks, although they are tiny, are observed, and these q values are also assigned to $1:3^{1/2}:7^{1/2}$. These results are consistent with the well-known fact that the SI diblock copolymer with a volume fraction of PS of either 0.26 (SIZ-4) or 0.65 (SIZ-3) has cylindrical microdomains.[30,31] Thus, it is concluded that both SIZ-3 and SIZ-4 have cylindrical morphologies at temperatures above the glass transition temperature of PS blocks. It should be noted here that the $4^{1/2}$ peak is not discernible in both SAXS profiles. The scattering comprises contributions from inter- and intraparticle interferences, and these are referred to as *lattice* and *particle* scattering, respectively. Since the particle scattering exhibits alternating constructive and destructive interferences, depending on the size and shape of the particle, the diffraction peak (lattice scattering peak) disappears when its angular position coincides with that of the destructive interference of the particle scattering. The extinction condition is governed by the volume fraction of particles in the system. For the hexagonally packed cylinders, Hashimoto et al.[29] have shown theoretically, by taking into account paracrystalline distortion, that the $4^{1/2}$ peak almost disappears when the volume fraction is around 0.274. For SIZ-4 with $\phi_{PS} = 0.26$, the $4^{1/2}$ peak is not observed due to the extinction condition. On the other hand, for SIZ-3 with $\phi_{PS} = 0.65$, the extinction condition for the $4^{1/2}$ peak is not satisfied. The $3^{1/2}$ peak should disappear according to the extinction condition for the volume fraction of roughly 0.326 (=1 − 0.674), which was demonstrated by Hashimoto et al.[29] The reason that the $4^{1/2}$ peak is not observed for SIZ-3 is unclear at present.

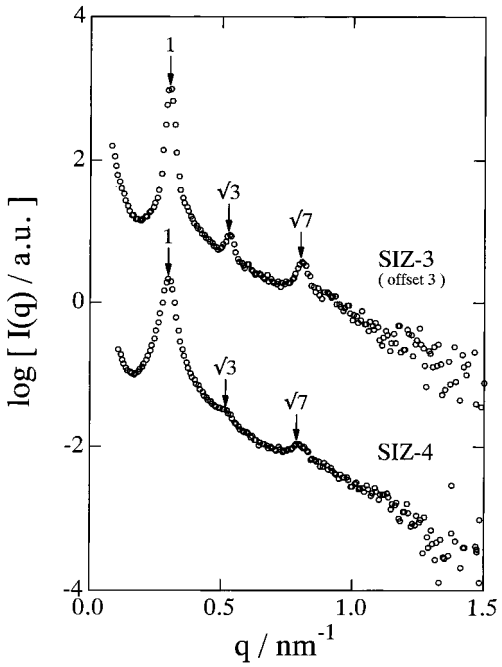

Figure 2. SAXS profiles [log $I(q)$ vs q] for neat block copolymers of SIZ-3 and SIZ-4 measured at room temperature, where the profile for SIZ-3 is vertically shifted by a factor of 3 to avoid overlap. Here, q and $I(q)$ are the magnitude of the scattering vector and the scattering intensity, respectively. Note that the SIZ-3 and SIZ-4 were annealed at 150 °C for 20 h and 110 °C for 26 h prior to the SAXS measurement.

Figure 3 gives SAXS profiles for the blends with three different overall volume fractions of polystyrene block in the blend ($\overline{\phi_{PS}}$): 0.41, 0.44, and 0.51. Samples were annealed either at 150 °C or at 200 °C for 20 h before SAXS measurements at room temperature. Note that the SAXS profiles for samples annealed at 150 °C are vertically shifted by a factor of 3 to avoid overlap. It

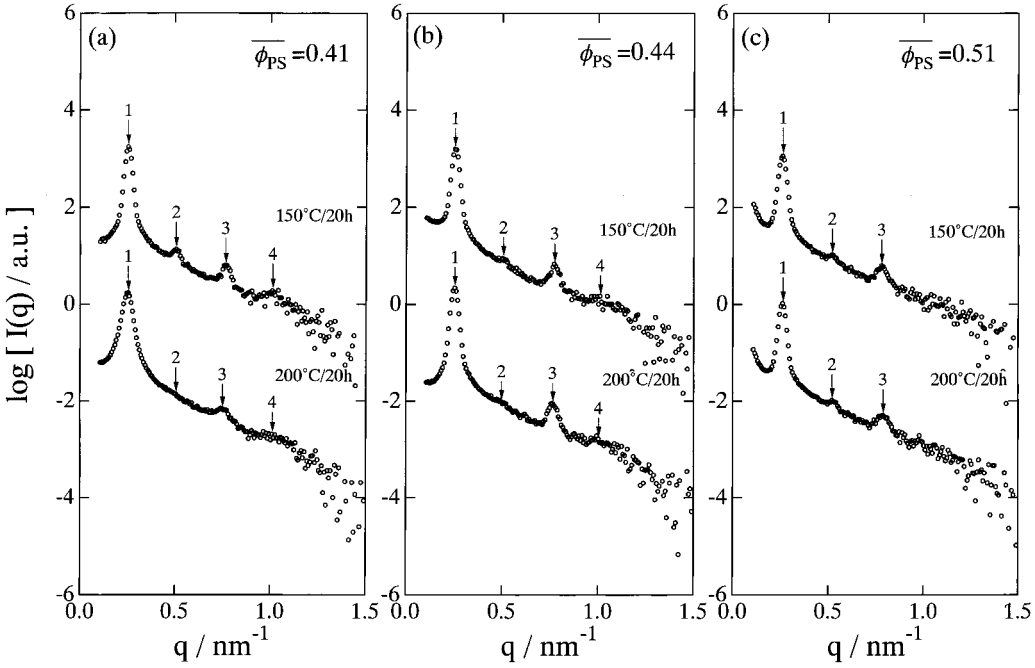

Figure 3. SAXS profiles for the binary blends of SIZ-3 and SIZ-4 with three different overall volume fractions of polystyrene blocks in the blend ($\overline{\phi_{PS}}$): (a) 0.41, (b) 0.44, and (c) 0.51. All samples were annealed at 150 and 200 °C for 20 h before SAXS measurements at room temperature. Note that the SAXS profiles for samples annealed at 150 °C are vertically shifted by a factor of 3 to avoid overlap.

can be clearly seen that diffraction peaks appear at the relative angular positions of 1:2:3:4 in each profile, which indicate a lamellar morphology. Thus, only lamellar morphology exists for the blends with $\overline{\phi_{PS}}$ ranging from 0.41 to 0.51, and any transition to other morphologies does not occur at temperatures up to 200 °C. Because two neat block copolymers of SIZ-3 and SIZ-4 exhibit cylindrical morphologies, the lamellar morphology found at these blends was formed through a mechanism similar to that shown in Figure 1a. It is noted in Figure 3 that the second-order peak is weak or almost absent as compared to the third-order peak in each sample. For a lamellar morphology, the extinction condition is governed by the relative ratio of the thicknesses of A and B lamellae, i.e., the volume fraction of block A (f) in the A−B diblock copolymer. It is theoretically shown that, when the nth order diffraction peak disappears, f can be estimated as m/n, where m is a natural number smaller than n.[32] According to this criterion, $f = 0.5$ ($m = 1$ and $n = 2$) for a block copolymer where the second-order peak is absent. However, the $\overline{\phi_{PS}}$ values of the samples employed in Figure 3 are not exactly identical to 0.5. Since the values of $\overline{\phi_{PS}}$ indicated in Figure 3 are estimated by assuming a uniform mixing of SIZ-3 and SIZ-4 copolymers, the fact that the SAXS profiles in Figure 3 imply $\overline{\phi_{PS}} \cong 0.5$, suggests more or less inhomogeneous distribution.

Figure 4 shows SAXS profiles measured at room temperature for the blend with $\overline{\phi_{PS}} = 0.60$ after annealing at various conditions. To avoid overlap, the SAXS profiles in Figure 4a for the blends annealed at 150 and 175 °C for 20 h are shifted vertically downward by a factor of 2 and 4, respectively. It can be seen in Figure 4a that, for the as-cast sample, two distinct peaks are observed at relative positions of 1:2, corresponding to a lamellar morphology. This is consistent with the result that the neat SI copolymer with the PS block volume fraction of 0.6 has lamellar microdomains.[30] However, due to the relatively broad peaks, the lamellar structure of the sample is considered to be ill-ordered. Nevertheless, because the SIZ-3 and SIZ-4 copolymers form PI cylinders and PS cylinders, respectively, these results imply that both of the component diblock copolymers are mixed together without any macroscopic phase separation. On the other hand, in the SAXS profiles for the blends annealed at 150 and 175 °C for 20 h, five scattering peaks were discernible at positions marked with symbols a−e, although peak b is more or less a shoulder in the profiles. The position and the intensity of these peaks are compared with theoretical predictions for the scattering arising from a gyroid morphology. Since the gyroid has $Ia\bar{3}d$ cubic symmetry of the space group, the relative peak position and intensity ratio corresponding to each higher order peak can be predicted and are given in Table 2, where those obtained from the observed peaks a−e are also summarized. From the results in Table 2, the observed relative peak positions are in excellent agreement with the predicted ones. Moreover, the ratios of the scattering intensities corresponding to higher order peaks agree approximately with predicted values obtained by Hajduk et al.[18] and by Matsen and Schick[16] for a gyroid morphology with 33 vol % of the minority phase. It is worthwhile to compare the experimental results with theoretical predictions for an ordered bicontinuous double diamond (OBDD) morphology with 33 vol % of the minority phase, where the q ratio and the intensity ratio of the first- to the second-order diffraction peaks are 1:1.22 ($=2^{1/2}:3^{1/2}$) and 1:0.352, respectively.[18] Therefore, it can be concluded that the morphology of the blend at 150 and 175 °C is a gyroid, not an OBDD, and the transition from lamellar to gyroid morphology took place upon annealing at 150 and 175 °C. On the other hand, it can be seen in Figure 4b that, for the blend annealed at 200 °C for 20 h, four peaks clearly appear at positions relatively assigned as $1:4^{1/2}:7^{1/2}:9^{1/2}$ which

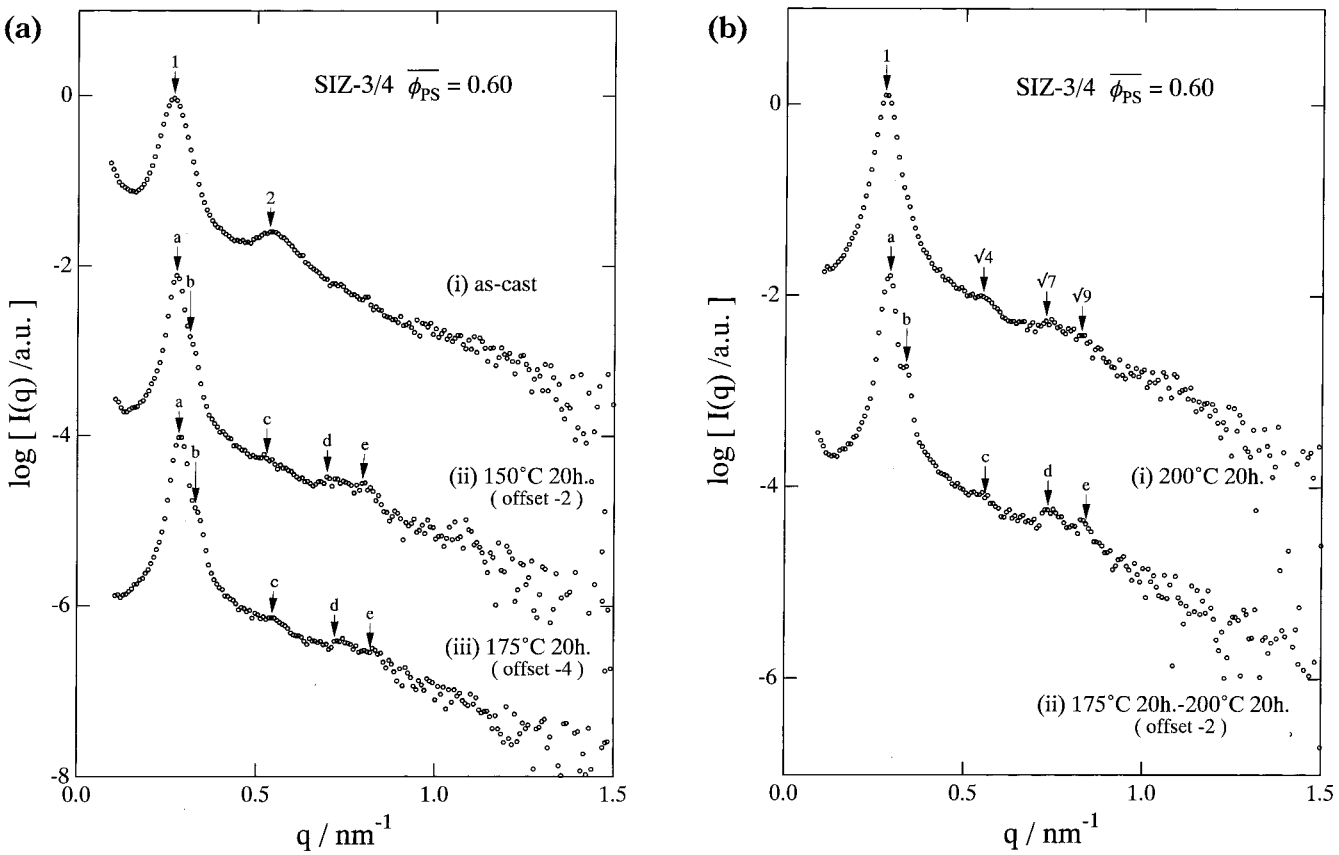

Figure 4. (a) SAXS profiles measured at room temperature for the blend with $\overline{\phi_{PS}} = 0.60$ at different annealing conditions: (i) as-cast, (ii) annealed at 150 °C for 20 h, and (iii) annealed at 175 °C for 20 h. To avoid overlap, the profiles for 150 and 175 °C for 20 h were shifted downward by a factor of 2 and 4, respectively. (b) SAXS profiles measured at room temperature for the blend with $\overline{\phi_{PS}} = 0.60$ at two different annealing conditions: (i) directly annealed at 200 °C for 20 h and (ii) first annealed at 175 °C for 20 h and further annealed at 200 °C for 20 h. The latter profile was shifted downward by a factor of 2 to avoid overlap.

Table 2. Lattice Scattering Peaks for Gyroid ($Ia\bar{3}d$)

			relative peak position		ratio of scattering intensity			
					exptl result			
peak	reflection[a]	modulus[b]	pred	obsd[c]	150 °C	175 °C	pred[d]	pred[e]
a	(211)	$6^{1/2}$	1.00	1.00	1.000	1.000	1.000	1.000
b	(220)	$8^{1/2}$	1.15	1.15	0.190	0.149	0.168	0.10957
c	(332)	$22^{1/2}$	1.91	1.91	0.0071	0.0076	0.008	0.00206
d	(532)	$38^{1/2}$	2.52	2.52	0.0043	0.0040	unknown	0.00246
d	(611)	$38^{1/2}$	2.52	2.52	0.0043	0.0040	unknown	0.00524
e	(550)	$50^{1/2}$	2.89	2.89	0.0036	0.0030	unknown	unknown

[a] Determined from extinction condition for $Ia\bar{3}d$ symmetry of space group.[36] [b] Modulus is defined for reflection (hkl) as $(h^2 + k^2 + l^2)^{1/2}$. [c] For both 150 and 175 °C. [d] Calculated for 33 vol % of a minority component assuming the *constant thickness structure* introduced by Hajduk et al.[18] [e] Calculated for 33 vol % of a minority component including the effect of chain asymmetry (difference in the statistical segment length) for SI diblocks from the self-consistent-field theory (given by Matsen and Schick[16]).

are the diffraction peaks from hexagonally packed cylinders.[29] This indicates that, when the as-cast sample was directly annealed at 200 °C, the morphological transition from lamellar to cylindrical microdomains occurred, although the existence of a gyroid phase during the transition is not completely excluded. It is noted that the $3^{1/2}$ peak for the blend annealed at 200 °C is not distinct. This is due to the fact that, for a block copolymer with hexagonally packed cylinder microdomains, the $3^{1/2}$ peak almost disappears when the volume fraction of one block is around 0.326 or 0.674.[29] The value of $\overline{\phi_{PS}}$ for this blend is 0.60, which is close to 0.674.

The above results lead one to speculate that a gyroid morphology could be transformed into cylindrical microdomains when the sample annealed at 150 (or 175 °C) is further annealed at 200 °C. To confirm this possibility, the SAXS experiment was conducted on the blend first annealed at 175 °C for 20 h, followed by annealing at 200 °C for 20 h, and the profile is given in Figure 4b, where five diffraction peaks are clearly observed at the marked positions a−e. This indicates that this sample has a gyroid morphology, which is deduced from the same argument applied to the SAXS profiles for the blend annealed at 150 and 175 °C in Figure 4a. Moreover, peak b in this sample is much more clearly observed compared with those in previous samples. Opposite to our speculation, the transition from a gyroid phase to cylindrical microdomains was not observed for the blend annealed first at 170 °C for 20 h, even if the additional annealing at 200 °C was done for 20 h. It may be considered that, once a gyroid

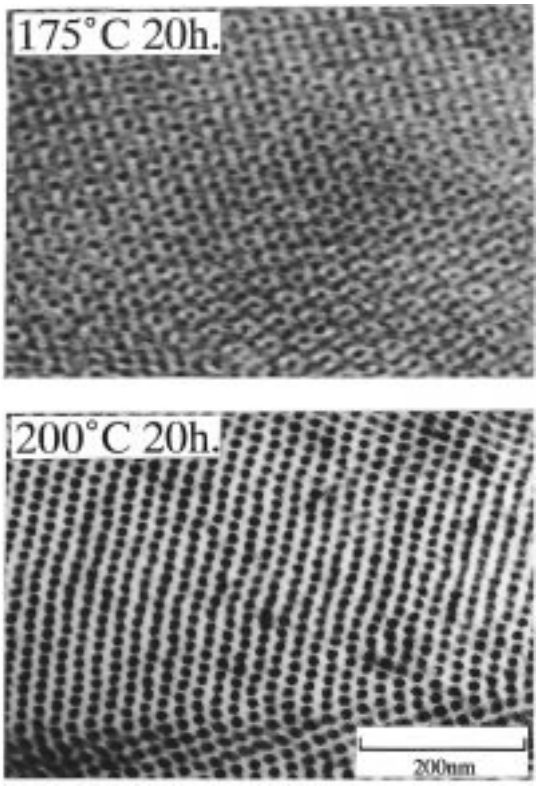

Figure 5. TEM micrographs for the blends with $\overline{\phi_{PS}} = 0.60$ annealed at 175 and 200 °C for 20 h. The dark region corresponds to the OsO_4-stained PI phase, and the bright one is for the unstained PS phase.

phase is formed, it is more difficult for it to be transformed into cylindrical microdomains, compared with the situation where preexisting lamellae are directly transformed into cylindrical microdomains. The gyroid is a three-dimensionally connected morphology, while a cylinder is a two-dimensional morphology. Since there is such mismatching of the connectivity, this may require enormous amounts of energy. It is known that morphological states depend on the history of thermal annealing.[33] Thus, it is still unclear that the cylindrical microdomains are the most stable morphology at 200 °C for the blend sample with $\overline{\phi_{PS}} = 0.60$. More sophisticated experiments are required to specify a stable morphology for the blend annealed at 200 °C.

To confirm the morphological structure complementarily, TEM observations were conducted. The TEM micrographs for the blends with $\overline{\phi_{PS}} = 0.60$ annealed at 175 and 200 °C for 20 h are displayed in Figure 5, where the dark region is the OsO_4-stained PI phase and the bright one is the unstained PS phase. The blend annealed at 175 °C for 20 h exhibits clearly the wagon wheel pattern, a typical bicontinuous microdomain structure.[6,15,18,23,24] However, it is not possible to exclude the possibility of an OBDD morphology from the TEM micrograph. The result of the TEM observation is simply a signature of the gyroid morphology for this sample, where the SAXS results shown in Figure 4a confirmed the gyroid. On the other hand, hexagonally packed cylinder microdomains are definitely seen in the TEM micrograph for the blend annealed at 200 °C for 20 h. But, a memory of lamellar morphology is widely detected in this image, where the PI cylinders are linearly arranged, in other words, packed in a distorted hexagonal lattice.

Figure 6 shows the SAXS profiles measured at room temperature for the blends with three different $\overline{\phi_{PS}}$ values, 0.57, 0.58, and 0.59, which were annealed at various temperatures for at least 20 h. A detailed explanation of the SAXS profiles for the blend with $\overline{\phi_{PS}} = 0.58$ is given in our previous paper.[15] Note that all SAXS profiles were obtained at PLS, Korea, except for two SAXS profiles corresponding to the blend with $\overline{\phi_{PS}} = 0.59$, annealed at 150 and 200 °C for 20 h. These two profiles were obtained at PF, Japan. It must be noted that the SAXS profiles were vertically shifted by a factor of 3 to avoid overlap. Note also here that the self-consistent field theory predicted the stability of the gyroid phase for a neat diblock copolymer at the compositional range around 0.58.[17] It can be seen in Figure 6a that the relative peak positions in the SAXS profile are expressed by 1:2 for the blend with $\overline{\phi_{PS}} = 0.57$ annealed at 120 and 130 °C, which is clear evidence of a lamellar morphology. Again, the homogeneous lamellar morphology implies that both of the component diblock copolymers in the blend are mixed together without macroscopic phase separation. On the other hand, the SAXS profile dramatically changed for this blend when it was annealed at 175 °C for 20 h. In addition to the disappearance of the lamellar second-order peak, a sharp peak appeared near the first-order peak. The ratio of peak positions can be expressed as 1:1.15 ($=6^{1/2}:8^{1/2}$), which corresponds to the reflections of (211) and (220) planes of a gyroid phase,[6,18,23,24,26] as discussed above (see also Table 2). As for the ratio of scattering intensity of these peaks, we found that our experimental result (1:0.111) agrees with theoretical values (1:0.110[16] or 1:0.168[18]) for a gyroid morphology with 33 vol % of minority phase. These results lead us to conclude that the morphological state of the blend with $\overline{\phi_{PS}} = 0.57$ at 175 °C is a gyroid. For this blend, annealed at 150 °C for 20 h, although the lamellar second-order peak is still distinct, a side peak is clearly observed at the relative peak position of 1.15, implying that the lamellar (L) and gyroid (G) phases coexist. Therefore, the temperature of 150 °C is close to the transition from L to G phase for the blend with $\overline{\phi_{PS}} = 0.57$. It can be seen in Figure 6b that, for the blend with $\overline{\phi_{PS}} = 0.58$, annealed at 140 °C for 20 h, a shoulder, although not a sharp peak, can be observed near the relative q position of 1.15, corresponding to a gyroid phase. This shoulder suggests that the annealing time of 20 h at 140 °C was not sufficiently long to develop a side gyroid peak due to very shallow quench (i.e., 140 °C might be very close to the transition temperature from L to G phase). Therefore, the temperature of 140 °C is close to the transition from L to G phase for the blend with $\overline{\phi_{PS}} = 0.58$. Details of kinetics of the transition for this blend are given in our previous paper.[15] It can be seen in Figure 6c that the blend with $\overline{\phi_{PS}} = 0.59$ exhibits a lamellar morphology at temperatures lower than 130 °C, and the gyroid morphology at temperatures higher than 150 °C, although the gyroid diffraction peak at the relative position of 1.15 is not very distinct.

Finally, on the basis of all the results given in Figures 3−6, an experimentally determined phase diagram in the vicinity of $\overline{\phi_{PS}} = 0.5$ is shown as a plot of χZ vs $\overline{\phi_{PS}}$ in Figure 7. Since, at the present time, there is no available expression for χ of the binary blends of block

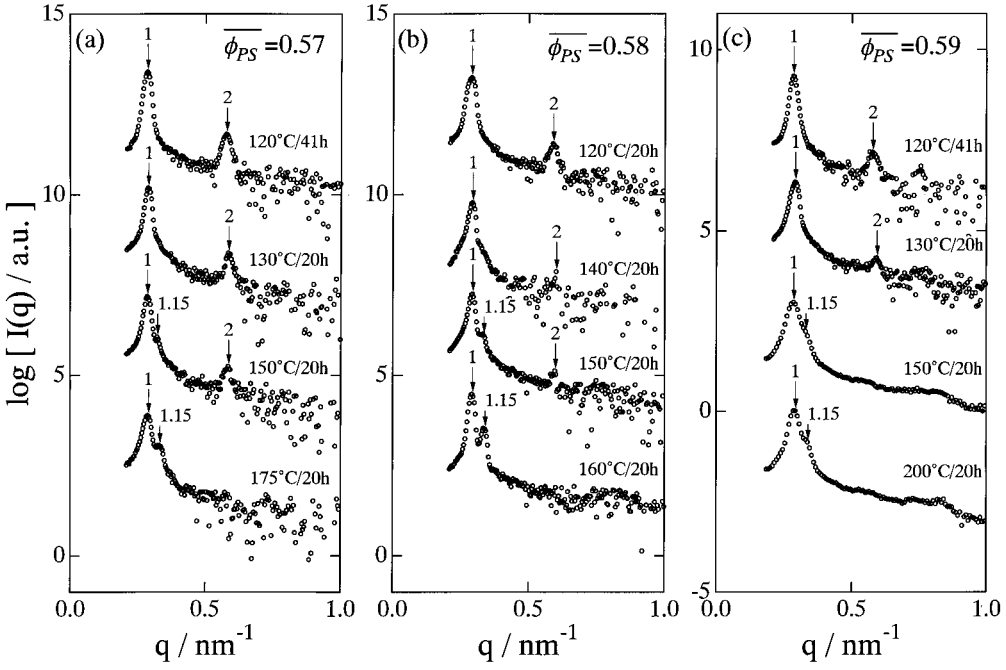

Figure 6. SAXS profiles measured at room temperature for the blends with three different $\overline{\phi_{PS}}$ values: (a) 0.57, (b) 0.58, and (c) 0.59. The blends were annealed at various temperatures for at least 20 h. Note that all SAXS profiles were obtained at PLS, Korea, except for two SAXS profiles corresponding to the blend with $\overline{\phi_{PS}}$ = 0.59, which were annealed at 150 and 200 °C for 20 h. These two profiles were obtained at PF, Japan. It must be noted that the SAXS profiles were vertically shifted by a factor of 3 to avoid overlap.

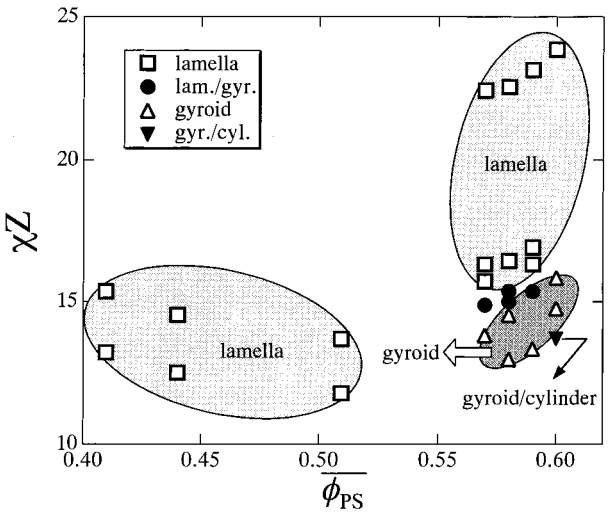

Figure 7. Phase diagram in the plots of χZ vs $\overline{\phi_{PS}}$, which is determined experimentally in the vicinity of ϕ_{PS} = 0.50. The value of χZ was estimated using eq 3. □, ●, △, and ▼ represent lamellar, lamellar/gyroid ill-defined states, gyroid, and gyroid/cylinder ill-defined states, respectively.

copolymers employed in this study, we estimated the value of χ for neat SI copolymers investigated recently by Mori et al.,[34] who found that χ depends on both the volume fraction of the PS blocks and the total molecular weight:

$$\chi Z = k_1 Z - k_2 + k_3 Z^{0.3}/T \qquad (3)$$

where k_1, k_2, and k_3 are constants depending on the volume fraction of the PS block (ϕ_{PS}) in an SI copolymer and T is the absolute temperature. For SI block copolymers with $\phi_{PS} \cong 0.5$, k_1 and k_2 are 9.11×10^{-3} and 6.91, respectively.[34] Also, from the results given in Figure 11 of ref 34, showing that k_3 is more likely a parabolic function of ϕ_{PS} with a minimum value at ϕ_{PS} = 0.5, we can estimate k_3 value at each value of ϕ_{PS}. For instance, the values of k_3 for the blends with ϕ_{PS} = 0.41, 0.44, 0.51, 0.57, 0.58, 0.59, and 0.60 are 1490, 1420, 1360, 1450, 1460, 1490, and 1520, respectively. In the phase diagram given in Figure 7, □, ●, △, and ▼ represent lamellar, lamellar/gyroid ill-defined states, gyroid, and gyroid/cylinder ill-defined states, respectively. It is interesting to find that a gyroid phase was not observed at $\overline{\phi_{PS}} < 0.5$; thus, a symmetry of the phase diagram with respect to $\overline{\phi_{PS}}$ = 0.5 for a gyroid phase is not satisfied. The asymmetry of the phase diagram may be ascribed to an inherent asymmetry in block chains of an SI diblock copolymer.[16] The chain asymmetry can be evaluated by the following expression:

$$\epsilon = \frac{f_A/f_B}{R_{g,A}^2/R_{g,B}^2} = \frac{v_A b_B^2}{v_B b_A^2} \qquad (4)$$

and ϵ is a quantitative measure of the chain asymmetry. Here, f_K, $R_{g,K}$, v_K, and b_K denote volume fraction, radius of gyration, segment molar volume, and the statistical segment length for K block (K = A or B), respectively. Note here that the values of v_K are 107.2 and 81.9 cm^3/mol and b_K are 0.67 and 0.65 nm for PS and PI, respectively.[27] Then, ϵ = 1.24 is evaluated (PS was chosen as A component).[35] Although some assumption may be required to compare the results, the phase diagram calculated for the case of b_A/b_B = 3/2 (Figure 5 in ref 16) by Matsen and Schick[16] exhibits a region of the gyroid phase for $\phi_A > 0.5$ that is farther away from ϕ_A = 0.5 than that for $\phi_A < 0.5$. If A would read to PI[37], their phase diagram should be flipped over with respect to ϕ_A = 0.5 when compared with our phase diagram, χZ vs $\overline{\phi_{PS}}$. Then, it turns out that another region for

the gyroid phase is expected at $\overline{\phi_{PS}} < 0.4$. To confirm experimentally this fact, the morphologies at $\overline{\phi_{PS}} < 0.4$ should be examined carefully. Although it has been shown theoretically that a region of a gyroid phase exists for a neat diblock copolymer,[16,17] clear experimental evidence for this morphology is not often presented, except for results from a few research groups[6,15,18,23−26] Although some research groups developed theories to allow one to predict the phase behavior for a binary blend of diblock copolymers,[10,13,14] there is no theory available which can predict a gyroid phase for a binary blend of block copolymers.

IV. Concluding Remarks

The morphology and phase behaviors of the binary blend of diblock copolymers were studied by small-angle X-ray scattering. In this blend, long and short block chains anchored to the interface are coexisting in the same microdomain space. The microdomain morphology can be controlled by adjusting the overall volume fractions of the PS block in the blend ($\overline{\phi_{PS}}$). This behavior is very similar to that of a neat block copolymer whose morphology depends upon the volume fraction of the PS block, ϕ_{PS}. However, some interesting results were obtained. One of these is for a lamellar structure. A more or less inhomogeneous distribution of SIZ-3 and SIZ-4 diblock copolymers was suggested. A morphological transition from lamellae to gyroid upon heating was clearly observed for the range of $0.57 \leq \overline{\phi_{PS}} \leq 0.60$. These results are consistent with speculation that the intradomain segregation or clustering of a major component in the microdomain space can reduce the energy barrier for the thermotropic transition. A phase diagram of the blend in the vicinity of $\overline{\phi_{PS}} = 0.5$ was experimentally obtained by plotting χZ vs ϕ_{PS}. We found that a gyroid phase was not observed at $0.40 < \overline{\phi_{PS}} < 0.50$; thus, the symmetry of a gyroid with respect to $\phi_{PS} = 0.5$ is not satisfied. This phase diagram would be very helpful in developing a theory for predicting order-to-order transition for the binary blend of block copolymers. The thermoreversibility of the transition between lamellar and gyroid phases was not confirmed in this study. However, it does not necessarily mean that the lamellar morphology is not stable at lower temperatures, because the reverse transition from G to L might be kinetically prohibited more than the forward transition (from L to G) in the binary blends of diblock copolymers.

Acknowledgment. We thank Mr. T. Fukui (Nippon Zeon Co., Ltd.) for kindly supplying the SI samples. This work was financially supported by Grants-in-Aid from the Japan Ministry of Education, Science, Culture, and Sports, with No. 07236228 to S.N. (Priority Areas "Cooperative Phenomena in Complex Liquids") and No. 08751048 to S.S. The time-resolved SAXS measurements were conducted under the approval of the Photon Factory Advisory Committee (Proposal No. 94G284). Synchrotron SAXS experiments were in part performed at the PLS, which was supported by Korean Ministry of Science and Technology (MOST) and Pohang Iron & Steel Co. (POSCO).

References and Notes

(1) Hashimoto, T.; Yamasaki, K.; Koizumi, S.; Hasegawa, H. *Macromolecules* **1993**, *26*, 2895.
(2) Spontak, R. J. *Macromolecules* **1994**, *27*, 6363.
(3) Spontak, R. J.; Fung, J. C.; Braunfeld, M. B.; Sedat, J. W.; Agard, D. A.; Ashraf, A.; Smith, S. D. *Macromolecules* **1996**, *29*, 2850.
(4) Spontak, R. J.; Fung, J. C.; Braunfeld, M. B.; Sedat, J. W.; Agard, D. A.; Kane, L.; Smith, S. D.; Satkowski, M. M.; Ashraf, A.; Hajduk, D. A.; Gruner, S. M. *Macromolecules* **1996**, *29*, 4494.
(5) Kane, L.; Satkowski, M. M.; Smith, S. D.; Spontak, R. J. *Macromolecules* **1996**, *29*, 8862.
(6) Laurer, J. H.; Hajduk, D. A.; Fung, J. C.; Sedat, J. W.; Smith, S. D.; Gruner, S. M.; Agard, D. A.; Spontak, R. J. *Macromolecules* **1997**, *30*, 3938.
(7) Sakurai, S.; Umeda, H.; Yoshida, A.; Nomura, S. *Macromolecules*, **1997**, *30*, 7614.
(8) Floudas, G.; Vlassopoulos, D.; Pitsikalis, M.; Hadjichristidis, N.; Stamm, M. *J. Chem. Phys.* **1996**, *104*, 2083.
(9) Almdal, K.; Rosedale, J. H.; Bates, F. S. *Macromolecules* **1990**, *23*, 4336.
(10) Yamaguchi, D.; Hashimoto, T.; Han, C. D.; Baek, D. M.; Kim, J. K.; Shi, A.-C. *Macromolecules* **1997**, *30*, 5832.
(11) Sakurai, S.; Nomura, S. *Polymer* **1997**, *38*, 4103.
(12) Zhao, J.; Majumdar, B.; Schulz, M. F.; Bates, F. S.; Almdal, K.; Mortensen, K.; Hajduk, D. A.; Gruner, S. M. *Macromolecules* **1996**, *29*, 1204.
(13) Shi, A.-C.; Noolandi, J. *Macromolecules* **1995**, *28*, 3103.
(14) Matsen, M. W.; Bates, F. S. *Macromolecules* **1995**, *28*, 7298.
(15) Sakurai, S.; Umeda, H.; Furukawa, C.; Irie, H.; Nomura, S.; Lee, H. H.; Kim, J. K. *J. Chem. Phys.*, in press.
(16) Matsen, M. W.; Schick, M. *Macromolecules* **1994**, *27*, 6761.
(17) Matsen, M. W.; Bates, F. S. *Macromolecules* **1996**, *29*, 1091.
(18) Hajduk, D. A.; Harper, P. E.; Gruner, S. M.; Honeker, C. C.; Kim, G.; Thomas, E. L.; Fetters, L. J. *Macromolecules* **1994**, *27*, 4063.
(19) Sakurai, S. *Trends Polym. Sci.* **1995**, *3*, 90.
(20) Hajduk, D. A.; Gruner, S. M.; Rangarajan, P.; Register, R. A.; Fetters, L. J.; Honeker, C.; Albalak, R. J.; Thomas, E. L. *Macromolecules* **1994**, *27*, 490.
(21) Sakurai, S.; Kawada, H.; Hashimoto, T.; Fetters, L. J. *Proc. Japan Acad. Ser. B* **1993**, *69*, 13.
(22) Sakurai, S.; Kawada, H.; Hashimoto, T.; Fetters, L. J. *Macromolecules* **1993**, *26*, 5796.
(23) Förster, S.; Khandpur, A. K.; Zhao, J.; Bates, F. S.; Hamley, I. M.; Ryan, A. J.; Bras, W. *Macromolecules* **1994**, *27*, 6922.
(24) Khandpur, A. K.; Förster, S.; Bates, F. S.; Hamley, I. M.; Ryan, A. J.; Bras, W.; Almdal, K.; Mortensen, K. *Macromolecules* **1995**, *28*, 8796.
(25) Sakurai, S.; Hashimoto, T.; Fetters, L. J. *Macromolecules* **1996**, *29*, 740.
(26) Hajduk, D. A.; Takenouchi, H.; Hillmyer, M. A.; Bates, F. S.; Vigild, M. E.; Almdal, K. *Macromolecules* **1997**, *30*, 3788.
(27) Fetters, L. J.; Lohse, D. J.; Richter, D.; Witten, T. A.; Zirkel, A. *Macromolecules* **1994**, *27*, 4639.
(28) Park, B. J.; Rah, S. Y.; Park, Y. J.; Lee, K. B. *Rev. Sci. Instrum.* **1995**, *66*, 1722.
(29) Hashimoto, T.; Kawamura, T.; Harada, M.; Tanaka, H. *Macromolecules* **1994**, *27*, 3063.
(30) Hasegawa, H.; Tanaka, H.; Yamasaki, K.; Hashimoto, T. *Macromolecules* **1987**, *20*, 1651.
(31) Koizumi, S.; Hasegawa, H.; Hashimoto, T. *Macromolecules* **1994**, *27*, 4371.
(32) Matsushita, Y.; Momose, H.; Yoshida, Y.; Noda, I. *Polymer* **1997**, *38*, 149.
(33) Pochan, D. J.; Gido, S. P.; Pispas, S.; Mays, J. W. *Macromolecules* **1996**, *29*, 5099.
(34) Mori, K.; Okawara, A.; Hashimoto, T. *J. Chem. Phys.* **1996**, *104*, 7765.
(35) Sakurai, S.; Hashimoto, T.; Fetters, L. J. *Macromolecules* **1995**, *28*, 7947.
(36) Hahn, T., Ed. *International Tables for X-ray Crystallography*, 3rd ed.; Kluwer Academic Publishers: Boston, MA, 1992; Part A, p 47.
(37) In ref 16, the ratio of Kuhn lengths is considered to be $b_{PI}/b_{PS} = 1.15$. Although we think, as stated in the text, that b_{PS} is almost identical to or rather slightly larger than b_{PI}, we follow the discussion on the asymmetric shape of the phase diagram as presented in ref 16 with $b_{PI} > b_{PS}$. It is needless to say that the shape of the asymmetric phase diagram with respect to $\overline{\phi_{PS}} = 0.5$ is contrary to our experimental result if $b_{PI} > b_{PS}$ would be assumed.

MA970471E